Parallel Hydrogenation for the Quantification of Wetting Efficiency and Liquid–Solid Mass Transfer in a Trickle-Bed Reactor

Arie Jan van Houwelingen and Willie Nicol
Dept. of Chemical Engineering, University of Pretoria, Pretoria 0002, South Africa

DOI 10.1002/aic.12342
Published online July 26, 2010 in Wiley Online Library (wileyonlinelibrary.com).

A novel method for the measurement of wetting efficiency in a trickle-bed reactor under reaction conditions is introduced. The method exploits reaction rate differences of two first-order liquid-limited reactions occurring in parallel, to infer wetting efficiencies without any other knowledge of the reaction kinetics or external mass transfer characteristics. Using the hydrogenation of linear- and isooctenes, wetting efficiency is measured in a 50-mm internal diameter, high-pressure trickle-bed reactor. Liquid–solid mass transfer coefficients are also estimated from the experimental conversion data. Measurements were performed for upflow operation and two literature-defined boundaries of hydrodynamic multiplicity in trickle flow. Hydrodynamic multiplicity in trickle flow gave rise to as much as 10% variation in wetting efficiency, and 10–20% variation in the specific liquid–solid mass transfer coefficient. Conversions for upflow operation were significantly higher in trickle-flow operation, because of complete wetting and better liquid–solid mass transfer characteristics. © 2010 American Institute of Chemical Engineers *AIChE J*, 57: 1310–1319, 2011
Keywords: trickle-bed reactors, liquid–solid mass transfer, wetting efficiency, multiphase reactors, hydrodynamics

Introduction

Packed bed reactors that process gas and liquid reactants are extensively used in industry, most notably in the petrochemical industry for hydroprocessing.[1,2] These reactors can be operated in gas–liquid cocurrent downflow (trickle flow), cocurrent upflow, or countercurrent flow. Because of the flexibility in terms of throughput, gas–liquid downflow reactors are often preferred when large process streams are involved.[3,4] The hydrodynamics of trickle flow are rather complex and upflow operation has been advocated for pilot-scale studies.[5] Existing studies on the comparison of upflow with trickle flow operation were summarized by Chaudari et al.,[6] who advocated systematic studies comparing these two operating modes; especially because several studies show possible advantages of upflow operation above trickle flow operation.

For hydroprocessing purposes, hydrodynamic parameters that influence mass transfer rates in the liquid phase are of particular importance.[4,7] These rates are primarily affected by the external liquid–solid mass transfer coefficient and wetting efficiency. Evidence of the influence of these parameters in reaction study is long in existence[2,8,9] and especially wetting efficiency received widespread attention in literature.

The most important measurement method is based on tracer measurements,[10–12] whereas several reaction methods were also suggested.[13–15] These methods use the additive model of Hartman and Coughlin,[13] which require an accurate kinetic description of the reaction. Other methods require correlations for liquid–solid mass transfer to estimate wetting

Correspondence concerning this article should be addressed to W. Nicol at willie.nicol@up.ac.za.

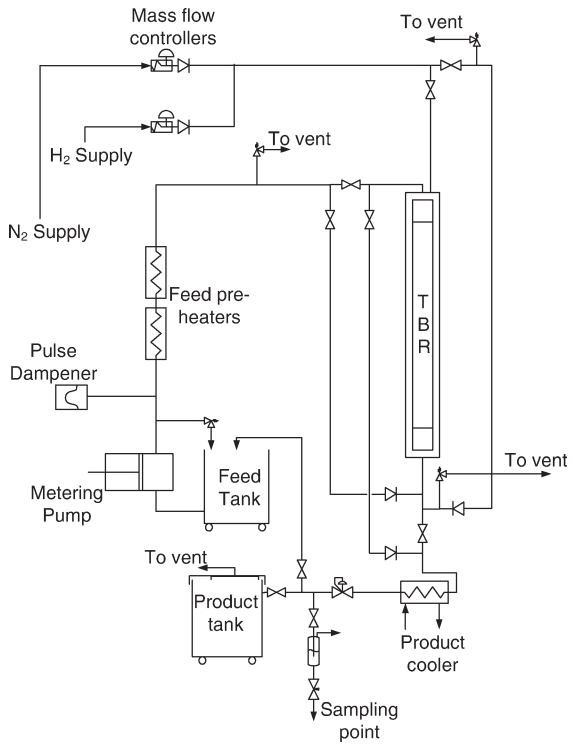

Figure 1. Schematic of the trickle-bed facility.

efficiency.[16,17] Recently, Baussaron et al.[18] generated an extensive amount of wetting efficiency data obtained from a colorimetric method, which was later expanded and correlated by Julcour-Lebigue et al.[19]

The overwhelming majority of liquid–solid mass transfer data in literature was obtained with either dissolution or an electrochemical technique. For the former, the packing material needs to be coated and is often not representative of a catalytic bed,[20] whereas for the latter the process fluid needs to be an electrolyte, limiting the applicability to typical process fluids.[21] There is a large deficiency of reactor-based measurements, especially at high pressures.[3]

In this work, a novel reaction method is presented for the measurement of wetting efficiency in a trickle-bed reactor. The method involves two reactions that are first order with respect to the nonvolatile, limiting reagents, occurring in parallel throughout the reactor. It is shown how the conversions (and relative difference) of the two reactions can be used to measure wetting efficiency without any other knowledge of the reaction kinetics and liquid–solid mass transfer coefficients. Mass transfer coefficients are also estimated from conversion data. Unlike for the wetting efficiency measurements, these estimations rely on an assumption regarding the general relationship between mass transfer coefficients and liquid superficial velocity.

Several studies report hysteresis in trickle flow, which is commonly attributed to the effect that flow history has on the liquid flow patterns in the bed.[22–24] Although subject of numerous studies, trickle flow multiplicity studies focus almost exclusively on pressure drop, liquid holdup, and flow texture.[23] Few studies exist that attempt to quantify the effect of flow history or prewetting on wetting efficiency[24] and liquid–solid mass transfer.[25] Moreover, direct studies of the effect of multiplicity on reactor performance are scarce.[26] In this investigation, two of the prewetting methods as summarized by van der Merwe and Nicol[27] are used to explore the boundaries of multiplicity behavior.

Approximations of the reported parameters are based on packed bed conversion data for two reactions: hydrogenation of linear octenes and hydrogenation of isooctenes (trimethylpentenes). This reaction system finds its application in the Fischer–Tropsch refining industry.[28] Fischer–Tropsch naphtha contains up to 85% olefins and requires severe hydrogenation. This leads to a drastic decrease in motor octane number (MON). The decrease in MON is highly dependent on the molecular structure of the hydrogenated olefin. As a rule, hydrogenation of linear olefins leads to a more severe drop in the octane number than the hydrogenation of branched olefins. Therefore, it is preferred to hydrogenate the branched olefins and retain the least branched olefinic molecules.

Experimental

Trickle-bed reactor setup

A flow sheet of the experimental setup is shown in Figure 1. The setup is designed to provide cocurrent gas–liquid upflow and downflow. The liquid reaction mixture, consisting of approximately 1% linear octene isomers and 2% isooctene isomers in a C_{14}–C_{20} paraffin solvent is pumped with a Bran & Luebbe H2-31 diaphragm metering pump, capable of delivering 70 l/min at 80 bar. Estimated properties of the liquid feed are given in Table 1. The liquid feed is preheated to the reaction temperature before entering a 50 mm internal diameter and 1000 mm length reactor. The reactor walls are temperature controlled using three external heaters with wall thermocouples. Eight internal thermocouples are used as illustrated in Figure 2 to measure internal temperatures and verify isothermal operation. A Rosemount model 3051CD differential pressure transmitter is used for pressure drop measurements to check for flow stability. In downflow operation, gas and liquid is distributed through a distributor plate with 21 4.5 mm holes, whereas liquid is distributed with 1/8 inch pipes that fits through these holes. In upflow operation, gas and liquid entering the bottom of the reactor is only distributed by a retaining sieve plate and the packing itself.

Nitrogen and hydrogen can be fed to the reactor, the flow rates being controlled by 0–30 Nl/min Brookes mass flow controllers. Maximum operating pressure of the system is 80 bar. A water-cooled heat exchanger is installed in the product line to cool down the product to approximately 30°C.

Table 1. Liquid Feed Properties

Property	Estimated Value	Estimation Method
Viscosity	1.71 mPa s	Van Velzen et al.[29] Kendall[30]
Surface tension	27 mN/m	Sugden[31]
Reagent molecular diffusivity in solvent		
Linear octenes	1.13×10^{-9} m^2/s	Wilke and Chang[32]
Isooctenes	1.13×10^{-9} m^2/s	
Average molar mass	~230 kg/kmol	Estimated from GC analysis

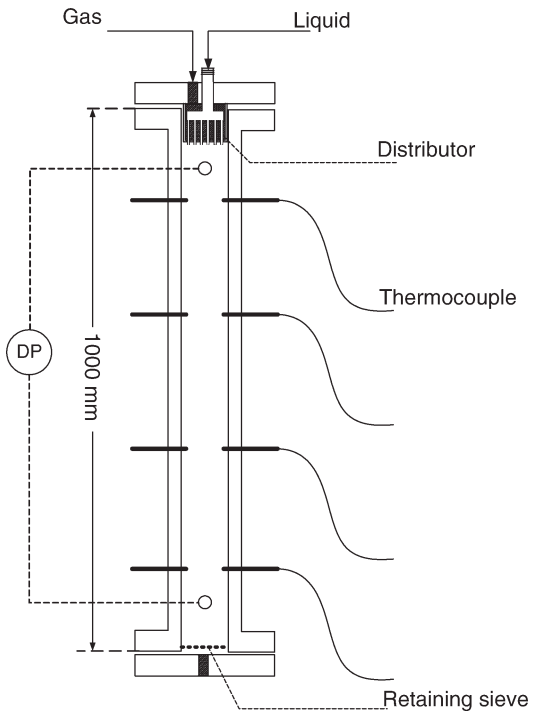

Figure 2. Reactor detail.

Pressure is regulated with a back-pressure regulator and monitored at strategic points in the system with pressure indicators and transducers. Samples are taken in a sampling bomb with dip tube for gas–liquid separation. Based on the high boiling points of the liquid components, it is clear that evaporation and entrainment of liquid product in the gas will not significantly affect the product composition at 30°C. The product stream can either be recycled to the feed tank or routed to the product tank.

Experimental conditions and procedure

For each experimental run, the olefins in the liquid feed was hydrogenated over a randomly packed bed of 0.3% Pd/γ-Al_2O_3 spherical eggshell catalyst diluted with γ-Al_2O_3 supports. All particles have a diameter of 3 mm and a catalyst shell thickness of 0.3 mm. All experiments were performed for five different liquid flow rates, corresponding to superficial velocities of 1.8, 2.6, 3.6, 4.5, and 7.5 mm/s, and three different flow configurations namely upflow, Levec prewetted trickle flow, and extensively prewetted trickle flow. The start-up procedure for each type of flow configuration is as follows:

- *Upflow*. The liquid flow is set to the required rate by adjusting pump stroke length and pump motor speed, and is fed to the bottom of the reactor, exiting at the top. Temperature control setpoints for the liquid feed preheaters and reactor heaters are set to the required temperatures. Nitrogen gas flow is introduced and the liquid is recycled to the feed tank until flow and temperature steady state has been reached. Once steady state is achieved, the product stream is rerouted to the product tank, nitrogen flow is shut off and hydrogen is introduced to the reactor. The feed tank is stirred, to ensure that the composition of the feed entering the reactor stays constant.
- *Levec prewetted trickle flow*. After the bed is flooded by feeding liquid in upflow, the liquid in the reactor is purged with nitrogen at atmospheric pressure, until no liquid can be detected in the reactor exit stream. The reactor is then pressurized with nitrogen to the required pressure, after which liquid is introduced to the top of the reactor at the required flow rate. It is ensured that the reactor pressure stays constant during the introduction of the liquid. The rest of the start-up procedure is the same as for upflow. For most hydrodynamic parameters, Levec prewetting represent the lower boundary of multiplicity in prewetted beds.[26]
- *Extensively prewetted trickle flow*. The reactor is flooded by feeding liquid at the required rate to the bottom of the reactor under recycle conditions, until no gas can be detected in the reactor exit stream. The liquid feed configuration is then changed from upflow to downflow, and nitrogen is introduced to the reactor. The rest of the start-up procedure is the same as for upflow. This prewetting procedure in most cases will result in operating on the upper boundary of the multiplicity envelope.[33]

Start-up procedures mentioned above require a measure for steady state, before nitrogen can be replaced by hydrogen. Steady state was verified by thermocouple readings, pressure drop, and flow rate measurements. Once temperature and pressure drop steady state is reached, the liquid product flow rate is repeatedly measured with a graduated cylinder and a stopwatch. If this stays constant, it is assumed that liquid holdup in the reactor stays constant and therefore hydrodynamic stability has been reached. This takes between 10 and 20 system residence times, depending on the flow rate and configuration. For each experiment, at least 50% stoichiometric excess of hydrogen is fed to the reactor. With the highest conversions reported in this article, this translates to 4.5 times the amount that has reacted. All downflow experiments were performed in the low interaction (trickle) flow regime. All experiments were performed at 60°C and 50 bar.

Two product samples were taken for each specific flow rate and configuration. The first sample is taken 10 reactor residence times (based on void volume) after achieving steady state, and the second three to five residence times later. The second sample serves to verify steady-state conditions in the reactor.

Samples were analyzed with an Agilent Technologies 6890 gas chromatograph (GC) fitted with a flame ionization detector. Elutriation was established on a 50-m long Pona column with a 0.2 mm inner diameter and a 0.5 mm film thickness with N_2 as carrier gas at a flow rate of 25 ml/min. A split ratio of 100:1 was used. The initial column temperature was 40°C, where it was held for 5 min. Then the temperature was ramped for 15 min at 4°C/min to obtain good separation of the C_8 reagents, after which the temperature is increased to 300°C at 25°C/min.

The catalyst bed consisted of 70 g of catalyst diluted with inert Al2O3 supports to achieve a total length of 630 mm. The bed is loaded between two layers of 140 mm inert support at the entrance and exit of the reactor. For a conversion of $X \leq 0.6$, the dispersion criterion of Sie and Krishna (1998) suggest a minimum reactor length of 550 mm for dispersion to be negligible in all modes of operation if the reaction is first order. Both the catalyst and support were supplied by Hereaus. Particle density was ± 1100 kg/m^3. Bed porosity was $\varepsilon \approx 0.4$ for all experiments.

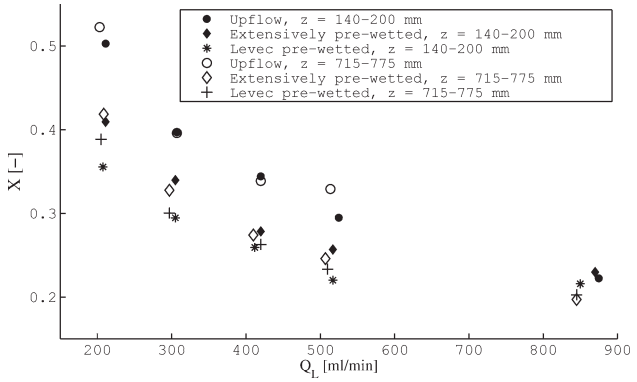

Figure 3. Test for saturation of liquid with hydrogen before entering the catalyst bed.

The quantity z refers to the position in the bed as measured from the top.

Gas mass transfer resistances and reaction order

Although the bulk of the reaction experiments were performed at the conditions as stated above, two other sets of experiments were also conducted. First of all, it has to be ensured that the liquid entering the bed is saturated with hydrogen, independent of liquid flow rate and flow configuration. For all experiments, 140 mm of inert supports were used to provide hydrogen saturation before entering the bed. It was verified experimentally that this amount of support is indeed enough to ensure saturation: Two experimental runs were performed, one with an undiluted (70 g) catalyst bed situated 140 mm from the top reactor inlet and another with the bed situated close to the bottom of the reactor (the depth of the bed was 715 mm to 775 m). The available area for gas–liquid mass transfer before entering the catalyst bed is far more in the former than in the latter case for gas–liquid upflow, and vice versa for trickle flow. Results for linear octane hydrogenation are shown in Figure 3. As these two runs agree satisfactorily for all experimental conditions, it can be assumed that the liquid is saturated with the gas before entering the bed. Both experiments were repeated with good repeatability.

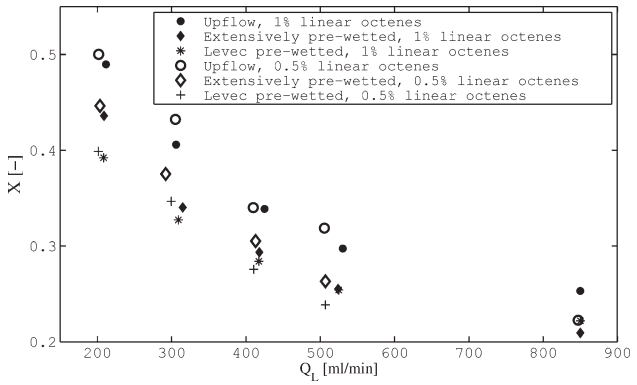

Figure 4. Conversion of linear octenes for feed concentrations of 0.5% and 1% linear octenes.

The feed also contained 0.5% and 2% isooctenes, respectively.

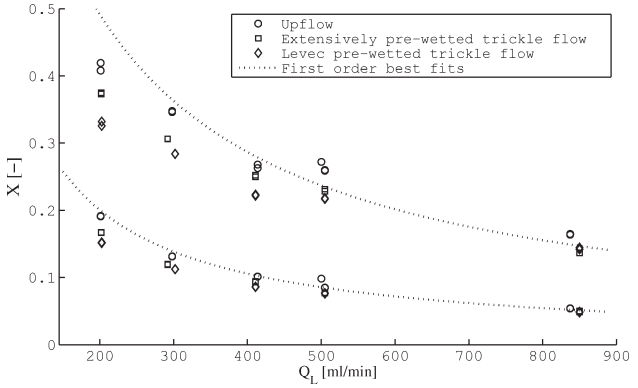

Figure 5. Typical conversion vs. flow rate dataset for an experimental run.

In another set of experiments, conversion data for the hydrogenation of a 1% linear octenes and 2% isooctenes feed were compared with hydrogenation of 0.5% linear octenes and 0.5% isooctenes. Results are shown in Figure 4. Close agreement between the results suggests that both reactions are liquid-limited and first order with respect to the liquid reagents; if gas mass transfer resistances play a role, conversions for the lower concentration feed would be higher than for the more concentrated feed. Hence, it can be assumed that the partial pressure of hydrogen was constant throughout the bed for all experiments, so that pseudo-first-order kinetics with respect to the liquid reagents can be assumed. Also, conversions that are independent of inlet concentration are characteristic for first-order reactions.

Results and Discussion

Conversion data

Typical conversion data for an experimental run is shown in Figure 5. In the rest of the discussion an "experimental run" will refer to two conversion data points for both reactions at five different liquid flow rates for all three different modes of operation. All the datapoints from an experimental run were generated consecutively (in no specific order) without interruption of the reactor temperature. Conversion data for the two different reactions are of course generated in parallel. The lower conversion data in Figure 5 is for isooctene hydrogenation, which is considerably slower than the hydrogenation of linear octenes. In total, nine experimental runs were performed, each consisting of a total of 60 conversion measurements (30 product samples for 15 different flow conditions and two reactions).

At all liquid flow rates and for both reactions, conversion decreases in the order: upflow $>$ extensively prewetted trickle flow $>$ Levec prewetted trickle flow at the same liquid flow rate. Although both reactions were established to be liquid-limited and first order in terms of the olefin concentration, none of the data show good first-order behavior for the fastest reaction and conversion rates increase with liquid flow rate. For the slower reaction (isooctene hydrogenation), the upflow conversion data approximates first-order behavior. These observations are clear indicators of liquid–solid mass transfer resistances, because the effective reaction rate

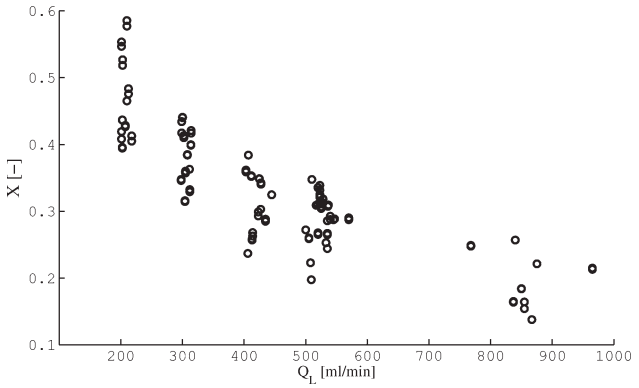

Figure 6. Unrefined upflow conversion data for the hydrogenation of linear octenes.

increases with liquid flow rate, and deviations from first-order behavior are more severe for the fast reaction. Hence, the following reactor model will be used in the treatment of upflow conversion data:

$$-\ln(1-X) = \frac{k_T V_{cat}}{Q_L} \tag{1}$$

$$k_T = \frac{k_R k_{LS} a}{k_R + k_{LS} a} \tag{2}$$

$$\text{where } a = \frac{6}{d_p};\quad V_{cat} = \frac{m_{cat}}{\rho_{cat}};\quad k_R = \eta_p k_r \tag{3}$$

The rate constant k_R in Eq. 2 includes the particle efficiency factor for a fully wetted particle, as shown in Eq. 3. Although upflow conversion data for the slower reaction approximates first-order behavior, significant deviations still persist in trickle flow at low liquid flow rates. The deviations from first-order behavior, even for the slower reaction, will be interpreted as a combined effect of resistance to mass transfer and incomplete wetting. If it is assumed that the area for liquid–solid mass transfer and the particle reaction rate (internal diffusion incorporated) is linearly dependent on the wetting efficiency, the apparent first-order rate constant is given by:

$$k_T = \frac{(f.k_R)(k_{LS}a.f)}{f.k_R + k_{LS}a.f} \quad = f\frac{k_R k_{LS} a}{k_R + k_{LS} a} \tag{4}$$

The assumption of linearity between the particle efficiency factor and wetting efficiency requires generalized particle moduli larger than 3[7]. For all experiments, the modulus for the fast reaction was determined to be larger than 10 based on shell volume and larger than 2.6 for the slower reaction. For this modulus, the maximum error in assuming a linear dependence of the particle efficiency on wetting efficiency is less than 1%.

Equation 4 will be used in the treatment of trickle flow conversion data. Note that for the rest of the discussion, k_T will be specific to each conversion datapoint. For example, k_{LS} and f are dependent on the hydrodynamics (i.e. upflow/downflow, liquid flow rate and used prewetting procedure). The liquid–solid mass transfer coefficient, k_{LS}, used in Eq. 4, is therefore not the same as in Eq. 3. The parameters in Eq. 4 that are independent of hydrodynamic conditions are k_R, which is specific to each reaction, and a, that is a function of the packing properties only.

Data refinement

Although all characteristics of Figure 5 were highly repeatable for most of the experimental runs, only a few experimental runs were quantitatively repeatable. An example of how conversion data varied from one experimental run to the other is shown in Figure 6. The large scatter is attributed to differences in catalyst activity. Two types of activity variations are possible: one where the catalyst activity varied within a run, and another where the catalyst was stable during a run, but at a different activity than during other experimental runs. Data from the former type of activity variation cannot be used, whereas data from the latter type can still be useful if treated correctly.

For selection of useful conversion data, first of all, it is necessary to discard all data from experimental runs during which the catalyst deactivated: catalyst deactivation while performing an experimental run might influence the interpretation of hydrodynamics. For indication of catalyst stability during an experimental run, the following catalyst activity indicator (CAI) was defined, which can be calculated from conversion data without any knowledge of the reaction rate constants (using the expression on the right):

$$\text{CAI} = \frac{k_{R1}.k_{R2}}{k_{R1} - k_{R2}} = \left.\frac{k_{T1}.k_{T2}}{k_{T1} - k_{T2}}\right|_{\text{upflow}} \tag{5}$$

The derivation of above equation is shown in Eqs. 7 and 8, which is used for the estimation of wetting efficiency. For complete wetting in the upflow mode, the CAI should be independent of liquid flow rate under liquid-limited conditions, and is directly related to the catalyst activity. All experimental runs during which the CAI decreased notably were discarded. An example of how the CAI is used is shown in Figure 7.

Because of the catalyst deactivation, data from four out of the nine experimental runs have to be discarded. Although all of the retained datasets are generated with stable catalyst, the stable catalyst activity varied from one experimental run to the other as shown in Figure 8. Therefore, it is important to develop methods for the estimation of the hydrodynamic parameters in Eqs. 1 and 4 that are insensitive to the specific catalyst activity.

Wetting efficiency

Consider two first-order reactions with particle rate constants k_{R1} and k_{R2} occurring in a trickle-bed reactor as modeled in Eq. 4. Using the effective rate constants k_{T1} and k_{T2} obtained from conversion data, the liquid mass transfer coefficient can be calculated twice for known reaction rate constants and wetting efficiency:

$$k_{LS}a = \frac{k_{T1}.k_{R1}}{f.k_{R1} - k_{T1}} = \frac{k_{T2}.k_{R2}}{f.k_{R2} - k_{T2}} \tag{6}$$

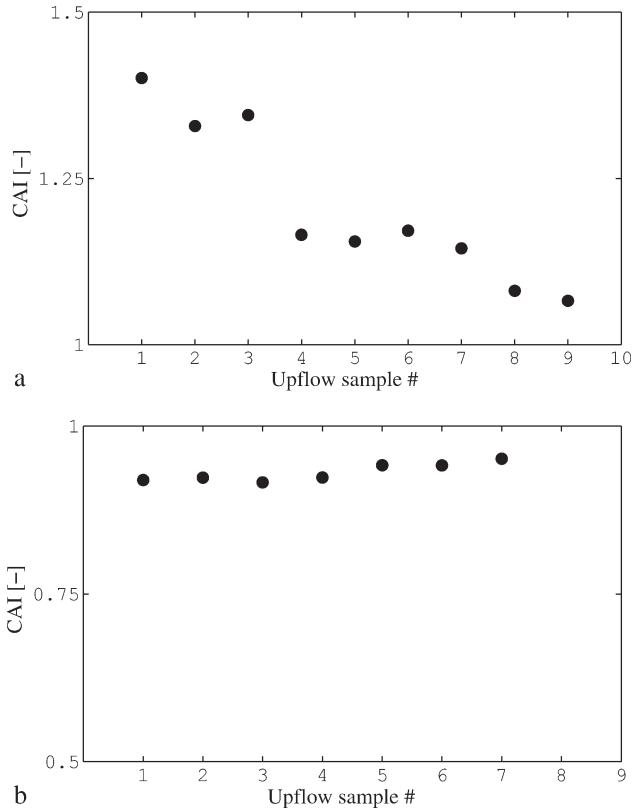

Figure 7. (a) An example of an experimental run for which the CAI indicates a drop in catalyst activity (all data generated during this run were discarded); (b) an example of an experimental run with stable catalyst.

The dataset generated during this run can be used.

Note that Eq. 6 is only valid if both reactions take place under the same hydrodynamic conditions, and refer to the treatment of one specific conversion datapoint. The relationship also relies on the assumption that the molecular diffusivities of both reagents are the same. According to the Wilke–Chang correlation, this assumption holds true for the current system (see Table 1).

By rearranging Eq. 6, it is possible to calculate wetting efficiency at a specific hydrodynamic state (mode of operation and liquid flow rate), if k_{R1} and k_{R2} is known.

$$f = \underbrace{\frac{k_{R1} - k_{R2}}{k_{R1}k_{R2}}}_{A} \times \underbrace{\frac{k_{T1}k_{T2}}{k_{T1} - k_{T2}}}_{B} \tag{7}$$

Part (A) of Eq. 7 contains only reaction rate constants and is constant for a stable catalyst. Therefore, part (B) of Eq. 7 is directly proportional to wetting efficiency and should be constant during upflow operation if the assumption of complete wetting in upflow holds true:

$$\frac{k_{R1} - k_{R2}}{k_{R1}k_{R2}} = \left.\frac{k_{T1} - k_{T2}}{k_{T1}k_{T2}}\right|_{upflow} \tag{8}$$

Comparing Eq. 8 with the definition of the CAI in Eq. 5, it was found that the CAI is a constant for stable catalyst or a function of time-on-stream only for an unstable catalyst as shown in Figure 7. Therefore, the wetting efficiency in upflow operation is constant and independent of liquid flow rate, and the assumption of complete wetting holds true. Therefore, wetting efficiencies in trickle flow operation can be calculated if conversion data is available for upflow operation at the same catalyst activity.

$$f_{TBR} = \left.\frac{k_{T1}k_{T2}}{k_{T1} - k_{T2}}\right|_{TBR} \times \left.\frac{k_{T1} - k_{T2}}{k_{T1}k_{T2}}\right|_{upflow} \tag{9}$$

Note that for the calculation of wetting efficiency, no knowledge of the kinetic rate constants k_{R1} and k_{R2} is required, and it is possible to calculate wetting efficiency from the raw conversion data as long as upflow conversion data for only and any one liquid flow rate is available at the same catalyst activity, i.e. the catalyst was stable during an experimental run. It is not necessary to have upflow conversion data available at all liquid flow rates: only one upflow conversion datapoint for both reactions is needed to calculate the quantity defined in Eq. 8, as long as the catalyst is stable. Figure 9 shows wetting efficiencies in trickle flow operation as calculated with Eq. 9. The averaged values for all experimental runs with stable catalyst are shown in Figure 10. As expected, hydrodynamic multiplicity is the most severe at low liquid velocities (±10–15% variation), where liquid flow in Levec prewetted beds tend to channel.[24] Wetting efficiency results for the Levec prewetted operation agree well with the correlation of Julcour-Lebigue et al.[19] The experimental data that was used in this correlation was generated in Levec prewetted beds.

Liquid–solid mass transfer

Contrary to the estimation of wetting efficiency, approximations of kinetic rate constants k_{R1} and k_{R2} are needed to estimate mass transfer rates from conversion data. For constant temperature, fluid properties, reagent diffusivity, and bed properties, most mass transfer correlations have the following functional relationship with liquid flow rate[3]:

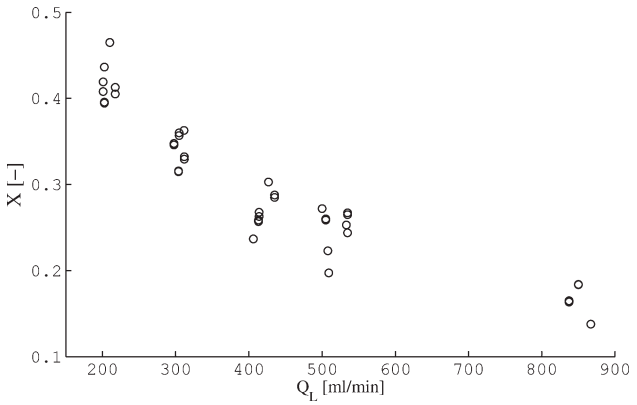

Figure 8. Upflow linear octene conversion data from experimental runs with stable catalyst.

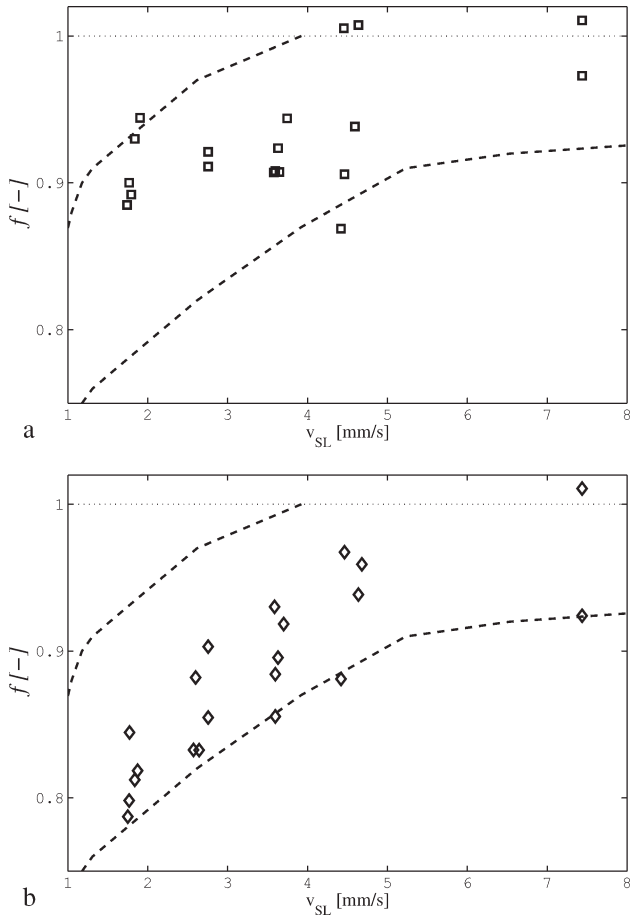

Figure 9. Wetting efficiencies as calculated from conversion data with Eq. 9 as a function of liquid superficial velocity.

Dotted lines indicate the estimations of wetting efficiency by Satterfield.[2] (a) Extensively prewetted trickle flow and (b) Levec prewetted trickle flow.

$$k_{LS}a = k_0 Q^{k1} \tag{10}$$

Based on this relationship the apparent rate constant at a specific liquid flow rate in upflow operation will, according to Eq. 4, be equal to:

$$k_{Tx,ij} = \frac{k_{Rx,i} k_0 Q_j^{k_1}}{k_{Rx,i} + k_0 Q_j^{k_1}} \tag{11}$$

where $x = 1$ for linear octene hydrogenation, $x = 2$ for isooctene hydrogenation, i refers to a specific experimental run and j refers to the liquid flow rate.

The coefficients k_0 and k_1 should be independent of the reaction rates, and the following function was minimized to obtain approximations of (a) kinetic rate constants for both reactions x and all experimental datasets i and (b) liquid–solid mass transfer for upflow operation as a function of liquid flow rate:

$$F = \sum_{xij} \left| X_{xij} + \exp\left(\frac{k_{Rx,i} k_0 Q_j^{k_1 - 1} . V_{cat}}{k_{Rx,i} + k_0 Q_j^{k_1}} \right) - 1 \right| \tag{12}$$

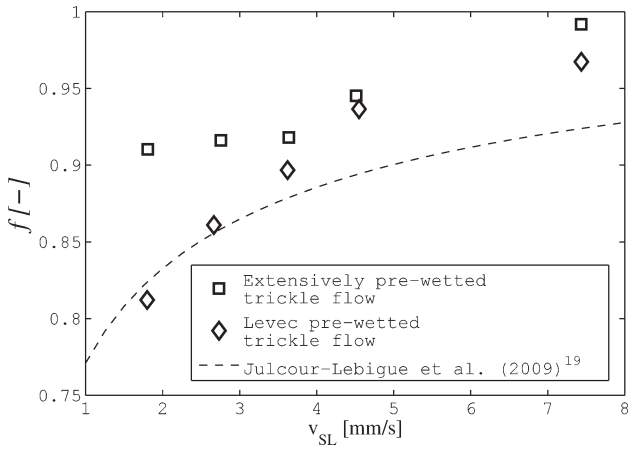

Figure 10. Averaged wetting efficiency for trickle flow operation as a function of liquid superficial velocity.

Minimization of this function is an iterative procedure, where $k_{Rx,i}$ is fitted onto conversion dataset i specific to reaction x with set values for k_0 and k_1 (one parameter fitted to ± 10 datapoints), and k_0 and k_1 is fitted to all conversion datasets with $k_{Rx,i}$ set for each dataset/reaction (two parameters fitted to ± 100 datapoints). Figure 11 shows datafits obtained with this procedure. Estimated values for k_{R1} and k_{R2} vary between 0.11 and 0.05, and 0.015 and 0.01 s^{-1}, respectively, based on catalyst volume.

As the particle kinetic rate constants are known, mass transfer coefficients can be calculated for all flow rates and operating modes by substituting Eq. 7 into Eq. 6:

$$k_{LS}a = \frac{k_{T1} - k_{T2}}{k_{T2}/k_{R2} - k_{T1}/k_{R1}} \tag{13}$$

With the wetting efficiency results from the wetting efficiency section, it is also possible to calculate mass transfer coefficients directly with Eq. 6. Equation 13 is preferred, so that mass transfer rates can be calculated without making use of the wetting efficiency results. Liquid–solid mass transfer

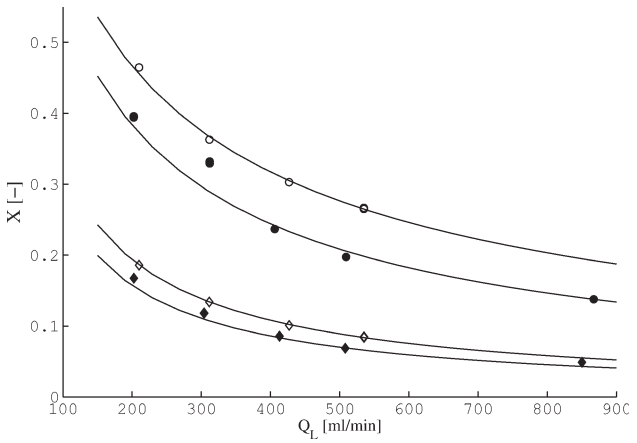

Figure 11. Fits of upflow conversion data obtained from minimizing Eq. 12.

The highest and lowest activity cases are shown.

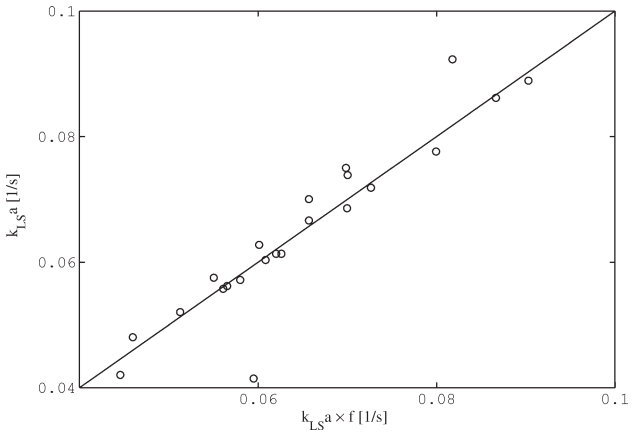

Figure 12. Parity plot for $k_{LS}a \times f$ and $k_{LS}a$ for upflow operation.

Good agreement confirms reasonability of estimated values for k_{R1} and k_{R2}.

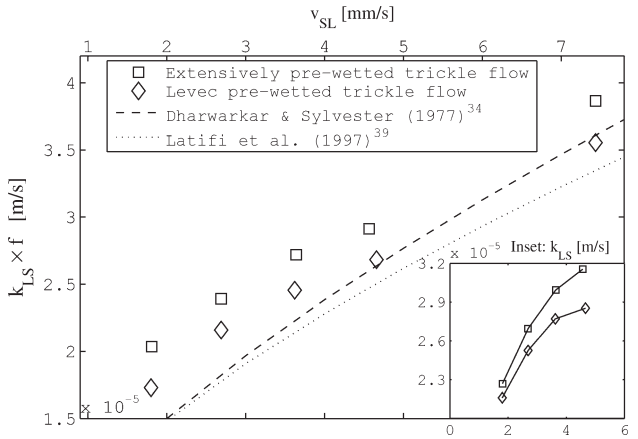

Figure 13. Averaged wetting efficiency-based liquid–solid mass transfer coefficients for trickle flow operation.

Inset: Specific mass transfer coefficients.

coefficients calculated with Eq. 13 are independent of the wetting efficiency and an indication of the specific rate of mass transfer at any specific point in the bed. Most liquid–solid mass transfer studies in trickle beds are based on either a dissolution method[20,34–36] or an electrochemical method.[25,37–40] These experimental methods lead to mass transfer coefficient measurements that include wetting efficiencies, i.e., usually $k_{LS} \times f$ is measured. To calculate $k_{LS} \times f$, one can once again use eqs. 6 and 7 to find the following relationship:

$$k_{LS}a.f = \frac{k_{R1} - k_{R2}}{k_{R1}/k_{T1} - k_{R2}/k_{T2}} \tag{14}$$

For upflow where $f = 1$, Eqs. 13 and 14 should yield the same results, which can be used as a test whether the estimated reaction rate constants are reasonable. This is indeed the case shown in Figure 12, which is a parity plot of upflow mass transfer rates calculated via Eqs. 13 and 14. Wetting efficiency-based ($k_{LS}f$, Eq. 14) and specific (k_{LS}, Eq. 13) liquid-solid mass transfer coefficients for trickle-bed operation are shown in Figure 13. Reported values are averages of five measurements. Overall, hydrodynamic multiplicity gave rise to about 10–20% variation in $k_{LS}f$. Literature correlations for dissolution-based[34] and electrochemical-based[39] mass transfer rate measurements are also shown in figure. The latter is recommended by Dudukovic et al.[3] for trickle-bed design purposes. However, many correlations predict liquid–solid mass transfer coefficients as much as 10 times smaller than that reported in the figure.

Previously, multiplicity of liquid–solid mass transfer in trickle beds has been explained as a combined liquid holdup–wetting efficiency effect.[26] At a specific superficial liquid velocity, a low liquid holdup should enhance mass transfer because of higher interstitial liquid velocities. On the other hand, low wetting efficiencies should be detrimental for mass transfer. The fact that liquid holdup (interstitial velocity) and wetting efficiency (area for mass transfer) are not the only hydrodynamic properties that influence mass transfer rates, is clear from the inset in Figure 13. Although the instantaneous mass transfer coefficients in this subfigure are not affected by wetting efficiency, a marked difference between Levec and extensively pre-wetted beds still persist. This finding is in direct agreement with the results from Joubert and Nicol[41] who observed slower liquid–solid mass transfer in a Levec prewetted bed than in an extensively prewetted bed, even though the interstitial velocity is higher (lower liquid holdup). This suggests that the difference in flow structure between the Levec and extensively prewetted beds[24,42–45] has a severe impact on the liquid–solid mass transfer characteristics.

Finally, liquid–solid mass transfer in trickle flow operation is compared to mass transfer in upflow operation as shown in Figure 14. Mass transfer coefficients in upflow are 12–30% higher for upflow operation than for trickle-flow operation at the same superficial liquid velocity, confirming that some flow characteristics in the trickle flow regime are detrimental for overall liquid–solid mass transfer rates. From the inset in Figure 14, it can be seen that the same trend applies for the specific mass transfer coefficient. The difference would have been more severe if interstitial velocity was

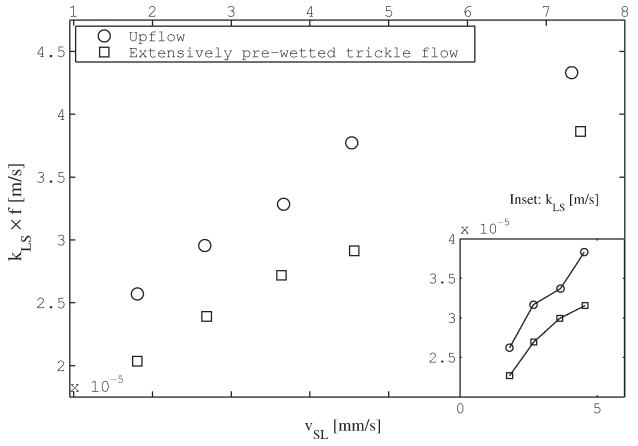

Figure 14. Comparison of liquid–solid mass transfer in trickle-flow and upflow operation.

Inset: Specific mass transfer coefficients.

used instead of superficial velocity, but due to the lack of holdup data, quantification could not be performed.

Conclusions

A novel parallel first-order reaction method was introduced to infer wetting efficiency in a trickle-bed reactor from conversion data of two liquid-limited reactions taking place in parallel in the reactor. The method is illustrated and validated by means of the parallel hydrogenation of linear- and isooctenes in a high pressure, 50 mm internal diameter trickle-bed reactor. Although previous reactor-based wetting efficiency measurement methods require an accurate estimation of the reaction rate constant(s), the current method only requires the reactions to be liquid-limited and first order. The exact magnitudes of the rate constants are of lesser importance, so that wetting efficiency measurements are insensitive to variations in catalyst activity. The same equations that are used to calculate wetting efficiencies can even be used to monitor catalyst stability. Wetting efficiency results were realistic and in agreement with literature. Liquid–solid mass transfer coefficients were also determined from the conversion data, by assuming a functional relationship between the liquid flow rate and liquid–solid mass transfer that is often encountered in literature. Two different prewetting procedures for trickle flow were investigated, to explore the boundaries of hydrodynamic multiplicity. Trickle flow results were also compared with upflow operation. The trickle flow multiplicity envelope shows up to 10% variation in wetting efficiency and 10–20% variation in mass transfer rates. Results suggest that different flow morphologies in trickle flow can have different effects on liquid–solid mass transfer. Overall, conversions for upflow were substantially higher for trickle flow operation, because of complete wetting and better specific liquid–solid mass transfer characteristics.

Acknowledgments

Sasol Research & Development and the National Research Foundation of South Africa are gratefully acknowledged for their financial support.

Notation

a = particle specific surface area ($a = 6/d_p$), 1/m
$_{d}p$ = particle diameter, m
f = wetting efficiency
η_p = pellet efficiency factor (for a fully wetted particle)
k_0 = fitting constant for upflow mass transfer (Eq. 10)
k_1 = fitting constant for upflow mass transfer (Eq. 10)
k_r = intrinsic first-order kinetic rate constant, based on particle density, 1/s
k_R = first-order particle kinetic rate constant based on particle density, 1/s
k_T = apparent first-order rate constant, 1/s
k_{LS} = liquid–solid mass transfer coefficient, m/s
m_{cat} = catalyst mass, g
Q_L = liquid flow rate, ml/min (in figures) or ml/s (in equations)
ρ_{cat} = catalyst particle density, g/ml
V_{cat} = total catalyst volume, ml
v_{SG} = gas superficial velocity, cm/s
v_{SL} = liquid superficial velocity, mm/s
X = conversion
z = bed depth, mm

Subscripts

1 = refers to linear octene hydrogenation
2 = refers to isooctene hydrogenation
i = refers to experimental run with stable catalyst
j = refers to specific liquid flow rate
x = refers to specific reaction

Literature Cited

1. Gianetto A, Specchia V. Trickle-bed reactors: state of art and perspectives. *Chem Eng Sci*. 1992;47:3197–3213.
2. Satterfield CN. Trickle bed reactors. *AIChE J*. 1975;21:209–228.
3. Dudukovic MP, Larachi F, Mills PL. Multiphase catalysis reactors: a perspective on current knowledge and future trends. *Catal Rev*. 2002;44:123–246.
4. Sie ST, Krishna R. Process development and scale up. III. Scale-up and scale-down of trickle bed processes. *Rev Chem Eng*. 1998;14:203–252.
5. De Wind M, Platenga FL, Heinerman JJL, Homanfree HW. Upflow versus downflow testing of hydrotreating catalysts. *Appl Catal*. 1988;43:239–252.
6. Chaudari RV, Jaganathan R, Mathew SP, Julcour C, Delmas H. Hydrogenation of 1,5,9-cyclodecatriene in fixed-bed reactors: down- vs. upflow modes. *AIChE J*. 2002;48:110–125.
7. Dudukovic MP. Catalyst effectiveness factor and contacting efficiency in trickle-bed reactors. *AIChE J*. 1977;23:940–944.
8. Henry HC, Gilbert JB. Scale up of pilot plant data for hydroprocessing. *Ind Eng Chem Process Des Dev*. 1973;12:328–334.
9. Sedriks W, Kenney CN. Partial wetting in trickle bed reactors the reduction of crotonaldehyde over a palladium catalyst. *Chem Eng Sci*. 1973;28:559–568.
10. Schwartz, JG, Wegwe, E, Dudukovic, MP. A new tracer method for determination of liquid–solid contacting effectiveness in trickle-bed reactors. *AIChE J*. 1976;22:894–904.
11. Colombo AJ, Baldi G, Sicardi S. Solid–liquid contacting effectiveness in trickle-bed reactors. *Chem Eng Sci*. 1976;31:1101–1108.
12. Mills PL, Dudukovic MP. Evaluation of liquid–solid contacting by tracer methods. *AIChE J*. 1981;27:893–903.
13. Hartman M, Coughlin RW. Oxidation of ethanol in gas–liquid cocurrent upflow and downflow reactors. *Chem Eng Sci*. 1972;27:867–880.
14. Ruecker CM, Ackgerman A. Determination of wetting efficiencies for a trickle bed reactor at high temperature and pressure. *Ind Eng Chem Res*. 1987;26:164–166.
15. Llano JJ, Rosal R, Sastre H, Diez FV. Determination of wetting efficiency in trickle-bed reactors by a reaction method. *Ind Eng Chem Res*. 1997;36:2616–2625.
16. Mata A, Smith JM. Transport processes in multiphase reactor systems. *AIChE Symp Ser*. 1981;77:29–35.
17. Goto S, Mabuchi K. Oxidation of ethanol in gas–liquid cocurrent upflow and downflow reactors. *Can. J. Chem. Eng*. 1984;62:865–869.
18. Baussaron L, Julcour-Lebigue C, Wilhelm A, Boyer C, Delmas H. Partial wetting in trickle-bed reactors: measurement techniques and global wetting efficiency. 2007;46:8397–8405.
19. Julcour-Lebigue C, Augier F, Maffre H, Wilhelm A, Delmas H. Measurements and modeling of wetting efficiency in trickle-bed reactors: liquid viscosity and bed packing effects. *Ind Eng Chem Res*. 2009;48:6811–6819.
20. Specchia V, Baldi G, Gianetto A. Solid–liquid mass transfer in concurrent two-phase flow through packed beds. *Ind Eng Chem Process Des Dev*. 1978;17:362–367.
21. Latifi MA, Laurent A, Storck A. Liquid–solid mass transfer in a packed bed with downward cocurrent gas–liquid flow: an organic liquid phase with high Schmidt number. *Chem Eng J*. 1988;38:47–56.
22. Kuzeljevic ZV, van der Merwe W, Al-Dahhan MH, Dudukovic MP, Nicol W. Effect of operating pressure on the extent of hysteresis in a trickle bed reactor. *Ind Eng Chem Res*. 2008;47:7593–7599.
23. Maiti R, Khanna R, Nigam KDP. Hysteresis in trickle-bed reactors: a review. *Ind Eng Chem Res*. 2006;45:5185–5198.
24. Van Houwelingen AJ, Sandrock C, Nicol W. Particle wetting distribution in trickle bed reactors. *AIChE J*. 2006;52:3532–3542.
25. Sims WB, Schulz FG, Luss D. Solid–liquid mass transfer to hollow pellets in a trickle bed. *Ind Eng Chem Res*. 1993;32:1895–1903.

26. Van der Merwe W, Nicol W, Al-Dahhan MH. Effect of hydrodynamic multiplicity on trickle bed reactor performance. *AIChE J*. 2008;54:249–257.
27. Van der Merwe W, Nicol W. Trickle flow hydrodynamic multiplicity: experimental observations and pore-scale capillary mechanism. *Chem Eng Sci*. 2009;64:1267–1284.
28. De Klerk A. Hydroprocessing peculiarities of Fischer–Tropsch syncrude. *Catal Today*. 2008;130:439–445.
29. Van Velzen D, Cardozo RL, Langenkamp H. A liquid viscosity–temperature–chemical constitution relation for organic compounds. *Ind Eng Chem Fundam*. 1972;11:20–25.
30. Kendall J. The viscosity of liquids. II. The viscosity–composition curve for ideal liquid mixtures. *J Am Chem Soc*. 1917;39:1787–1802.
31. Sugden S. A relation between surface tension, density, and chemical composition. *J Chem Soc Trans*. 1924;25:1177–1189.
32. Wilke CR, Chang P. Correlation of diffusion coefficients in dilute solutions. *AIChE J*. 1955;1:264–270.
33. Loudon DS, van der Merwe W, Nicol W. Multiple hydrodynamic states in trickle flow: quantifying the extent of pressure drop liquid holdup and gas–liquid mass transfer variation. *Chem Eng Sci*. 2006; 61:7551–7562.
34. Dharwarkar A, Sylvester ND. Liquid–solid mass transfer in packed beds. *AIChE J*. 1977;23:376–378.
35. Lakota A, Levec J. Solid–liquid mass transfer in packed beds with cocurrent downward two-phase flow. *AIChE J*. 1990;36:1444–1448.
36. Sylvester ND, Pitayagulsarn P. Mass transfer for two-phase cocurrent downflow in a packed bed. *Ind Eng Chem Process Des Dev*. 1975;14:421–426.
37. Chou TS, Worley FL, Luss D. Local particle–liquid mass transfer fluctuations in mixed phase cocurrent downflow through a fixed bed in the pulsing regime. *Ind Eng Chem Res*. 1979;18:279–283.
38. Hirose T, Mori Y, Sato Y. Liquid-to-particle mass transfer in fixed bed reactor with cocurrent gas–liquid downflow. *J Chem Eng Jpn*. 1976;9:220–225.
39. Latifi MA, Naderifar A, Midoux N. Experimental investigation of the liquid/solid mass transfer at the wall of a trickle-bed reactor-influence of Schmidt number. *Chem Eng Sci*. 1997;52:4005–4011.
40. Trivizadakis ME, Karabelas AJ. A study of local liquid/solid mass transfer in packed beds under trickling and induced pulsing flow. *Chem Eng Sci*. 2006;61:7684–7696.
41. Joubert R, Nicol W. Multiplicity behavior of trickle flow liquid–solid mass transfer. *Ind Eng Chem Res*. 2009;48:8387–8392.
42. Kan KM, Greenfield PF. Pressure drop and holdup in two-phase cocurrent trickle flows through beds of small packings. *Ind Eng Chem Process Des Dev*. 1979;18:740–745.
43. Lutran PG, Ng KM, Delikat EP. Liquid distribution in trickle beds. An experimental study using computer-assisted tomography. *Ind Eng Chem Res*. 1991;30:1270–1280.
44. Ravindra PV, Rao DP, Rao MS. Liquid flow texture in trickle-bed reactors: an experimental study. *Ind Eng Chem Res*. 1996;36:5133–5145.
45. Van der Merwe W, Nicol W, de Beer F. Trickle flow distribution by X-ray tomography. *Chem Eng J*. 2007;132:47–59.

Manuscript received Oct. 31, 2009, revision received Feb. 16, 2010, and final revision received Jun. 18, 2010.